Tight-binding bonding orbital model for third-order nonlinear optical susceptibilities in group-IV crystals

Karamjeet Arya*
International Center for Theoretical Physics, Trieste, Italy

Sudhanshu S. Jha
Tata Institute of Fundamental Research, Bombay 400005, India
(Received 25 October 1978)

The nonresonant part of the third-order nonlinear optical susceptibility $\chi^{(3)}$ has been calculated for diamond, silicon, and germanium by using the tight-binding Bloch states constructed from sp^3 hybridized orbitals. Only the nearest-neighbor bond interactions have been retained in the calculations. The three independent energy parameters, which enter in the model, are fitted by comparing the calculated and known experimental values of the valence-band width at $\vec{k} = 0$, the direct energy gap, and the linear dielectric constant. An explicit exponential form of the s- and p-type atomic orbitals is used in order to obtain the required dipole matrix elements in each case. Although the sign of the calculated $\chi^{(3)}$ agrees with the experimental values in each case, the agreement in magnitude of $\chi^{(3)}$ is best attained for diamond where the tight-binding model is expected to be very good.

I. INTRODUCTION

The induced electronic polarization field $\vec{P}$ in a solid, in general, contains both linear and nonlinear terms in the incident electromagnetic field $\vec{E}$. It can be symbolically written as

$$P_i = \sum_j \chi^{(1)}_{ij} E_j + \sum_{j,k} \chi^{(2)}_{ijk} E_j E_k + \sum_{j,k,l} \chi^{(3)}_{ijkl} E_j E_k E_l + \cdots , \quad (1)$$

where $\chi^{(1)}$, $\chi^{(2)}$, and $\chi^{(3)}$ are the linear, bilinear, and trilinear susceptibilities, respectively. The linear-electronic-response theory has been well known for a long time and has been studied extensively both experimentally and theoretically. However, in the optical region it became possible to measure $\chi^{(2)}$ and $\chi^{(3)}$ only after the availability of intense laser sources. The formal quantum-mechanical expressions for these susceptibilities for a crystal can be written in terms of the unperturbed electronic states of band theory. However, because of the difficulty in obtaining accurate unperturbed states, it became difficult to calculate these susceptibilities to yield any quantitative result for the nondispersive part. The dispersive part, however, may be calculated fairly accurately since this requires a detailed knowledge of the band structure only in a limited region of energy.

In order to obtain the nondispersive part of $\chi^{(2)}$ and $\chi^{(3)}$, having contributions arising from almost the whole Brillouin zone, several empirical calculations[1-4] have been made which approximately take into account the average band structure over the whole Brillouin zone (BZ). Although most of these models give reasonably good results for $\chi^{(2)}$ when appropriate parameters of the model are chosen properly, in many cases the results for $\chi^{(3)}$ differ considerably from their experimental values.[1,2] For group-IV crystals, a calculated value of $\chi^{(3)}$ is sometimes found to differ even in sign. Note that within the electric dipole approximation, $\chi^{(2)}$ is zero for group-IV crystals because of the center-of-inversion symmetry, while $\chi^{(3)}$ is nonzero.

In the completely-localized-bond approximation,[5] the electronic band structure in group-IV crystals is characterized by two fourfold-degenerate flat bands, referring to the valence and conduction bands. Corresponding electronic states are the bonding and antibonding wave functions for the four tetrahedral bonds, respectively. In this approximation,[1] the expression for $\chi^{(3)}$ consists of two terms, one negative term containing the dipole matrix elements only between bonding and antibonding states, and the other term which, in addition, contains matrix elements between bonding-bonding or antibonding-antibonding states. For group-IV crystals the second term, however, vanishes identically because of the center-of-inversion symmetry, thereby leading to a negative $\chi^{(3)}$. For crystals which do not have center-of-inversion symmetry, the second term is nonzero; but even then theoretical results[1] in this case for $\chi^{(3)}$ do not agree with the experimental values.

Using an involved molecular-orbital approach, Flytzanis[4] was able to obtain fairly good numbers, but Van Vechten and Aspnes[6] used a completely

different approach based on the intraband Franz-Keldysh effect to calculate $\chi^{(3)}$. They found that for crystals with small energy gaps intraband contributions become quite important. Using a simplified two-band model and the Kramers-Krönig relation, they calculated $\chi^{(3)}$ in some of the group-IV and III–V crystals and obtained a reasonable agreement with the experimental values. Within the framework of the band picture of the solid, which in principle includes the above contribution, we plan as an alternative approach to use a tight-binding bonding orbital model[7,8] in which all the interactions up to nearest-neighbor bonds are retained for calculating $\chi^{(3)}$ in group-IV crystals. In this model, the valence band consists of a twofold-degenerate flat band and two other nondegenerate bands whose energy depends on $\vec{k}$. Conduction bands also have a similar structure. This is discussed in Sec. II. Analytical expressions for the dipole matrix elements between different band states are also given in Sec. II.

In Sec. III we make explicit calculations for the nondispersive part of $\chi^{(3)}$ using the bonding orbital model. The three parameters entering into the energy-dispersion relations are fixed by comparing theoretical expressions with the experimentally known results for the valence-band width and direct energy gap at the Γ point and the linear dielectric constant. For calculating dipole matrix elements, we have used an exponential form of the s and p atomic orbitals recently used by Chadi[9] in his tight-binding calculations of the electronic band structure. The calculated values of $\chi^{(3)}$ for diamond and silicon are in good agreement with the experimental results, but, for germanium, the agreement is not so good. We discuss our results in Sec. IV.

II. TIGHT-BINDING BONDING ORBITAL MODEL

In the bonding orbital model, the eight valence electrons per unit cell in a group-IV crystal are accommodated in four equivalent tetrahedral bonds between adjacent atoms in crystallographic ⟨111⟩ directions (Fig. 1). For each bond we construct bonding and antibonding states $\psi^b_m(\vec{r})$ and $\psi^a_m(\vec{r})$, where $m = 1, 2, 3, 4$, respectively, by taking a linear combination of the atomic orbitals corresponding to two atoms forming the bond as

$$\psi^b_m(\vec{r}) = [1/(N_{bm})^{1/2}][\Phi_m(\vec{r}) + \Phi_m(-\vec{r} + \vec{t}_m)] , \tag{2}$$

$$\psi^a_m(\vec{r}) = [1/(N_{am})^{1/2}][-\Phi_m(\vec{r}) + \Phi_m(-\vec{r} + \vec{t}_m)] , \tag{3}$$

where

$$\vec{t}_1 = \tfrac{1}{4}a(\hat{i}+\hat{j}+\hat{k}),\quad \vec{t}_2 = \tfrac{1}{4}a(-\hat{i}-\hat{j}+\hat{k}),$$
$$\vec{t}_3 = \tfrac{1}{4}a(-\hat{i}+\hat{j}-\hat{k}),\quad \vec{t}_4 = \tfrac{1}{4}a(\hat{i}-\hat{j}-\hat{k}), \tag{4}$$

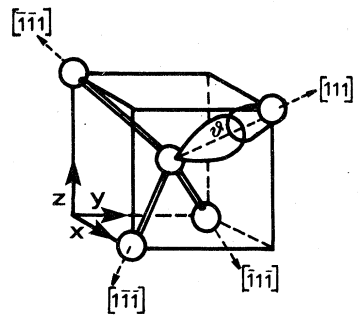

FIG. 1. Unit cells for the diamond crystal lattice showing the tetrahedral bonding. The balls represent the atoms.

a being a lattice constant. The normalization constants N_{bm} and N_{am} are given as

$$N_{bm} = 2 + 2S_{mm}, \tag{5}$$

$$N_{am} = 2 - 2S_{mm}, \tag{6}$$

$$S_{mn} = \langle \Phi_m(\vec{r}) \,|\, \Phi_n(-\vec{r} + \vec{t}_n) \rangle . \tag{7}$$

The four bonding orbitals Φ_m are constructed from sp^3 hybridized atomic orbitals in such a way that these point towards the four tetrahedral bonding directions

$$\Phi_1 = \tfrac{1}{2}(\phi_s + \phi_x + \phi_y + \phi_z), \tag{8}$$

$$\Phi_2 = \tfrac{1}{2}(\phi_s - \phi_x - \phi_y + \phi_z), \tag{9}$$

$$\Phi_3 = \tfrac{1}{2}(\phi_s - \phi_x + \phi_y - \phi_z), \tag{10}$$

$$\Phi_4 = \tfrac{1}{2}(\phi_s + \phi_x - \phi_y - \phi_z). \tag{11}$$

For this set of bonding orbitals, it can be shown that $S_{11} = S_{22} = S_{33} = S_{44} = S$.

In the tight-binding approximation, for any given $\vec{k}$ vector in the first BZ, the basic set of eight functions of the Bloch form can be taken as

$$\Psi^V_m(\vec{k}, \vec{r}) = \frac{1}{(\frac{1}{2}N)^{1/2}} \sum_j e^{i\vec{k}\cdot\vec{R}_j} \psi^b_m(\vec{r} - \vec{R}_j), \tag{12}$$

$$\Psi^C_m(\vec{k}, \vec{r}) = \frac{1}{(\frac{1}{2}N)^{1/2}} \sum_j e^{i\vec{k}\cdot\vec{R}_j} \psi^a_m(\vec{r} - \vec{R}_j), \tag{13}$$

where $\frac{1}{2}N$ is the number of unit cells in the crystal and $\vec{R}_j$ is the position of the jth cell. In the above basis set, the secular equation in terms of the matrix elements of the periodic crystal Hamiltonian H has the form

$$\det \begin{vmatrix} H^{VV}_{mn}(\vec{k}) - E(\vec{k})\Delta^{VV}_{mn} & H^{VC}_{mn}(\vec{k}) \\ H^{CV}_{mn}(\vec{k}) & H^{CC}_{mn}(\vec{k}) - E(\vec{k})\Delta^{CC}_{mn} \end{vmatrix} = 0 , \tag{14}$$

where

$$\Delta^{VV(CC)}_{mn}(\vec{k}) = \langle \Psi^{V(C)}_m(\vec{k}, \vec{r}) \,|\, \Psi^{V(C)}_n(\vec{k}, \vec{r}) \rangle , \tag{15}$$

$$H^{VV(CC)}_{mn}(\vec{k}) = \langle \Psi^{V(C)}_m(\vec{k},\vec{r}) | H | \Psi^{V(C)}_n(\vec{k},\vec{r}) \rangle , \quad (16)$$

$$H^{VC}_{mn}(\vec{k}) = \langle \Psi^{V}_m(\vec{k},\vec{r}) | H | \Psi^{C}_n(\vec{k},\vec{r}) \rangle . \quad (17)$$

In general, Eq. (14) involves the calculation of matrix elements of H and overlap integrals Δ between orbitals belonging to different unit cells in the crystal. This makes the calculations very difficult. However, if we make the simplifying assumption that interaction between any two bonds which do not have at least one atom common to them is neglected (i.e., retaining only nearest-neighbor bond interactions), the matrix elements can be written as

$$H^{VV}_{mn}(\vec{k}) = \exp[i\vec{k}\cdot(\vec{t}_m - \vec{t}_n)/2] \times[\beta_V \delta_{mn} + (1-\delta_{mn})\beta_{1V} \cos\vec{k}\cdot(\vec{t}_m - \vec{t}_n)/2] , \quad (18)$$

$$H^{CC}_{mn}(\vec{k}) = \exp[i\vec{k}\cdot(\vec{t}_m - \vec{t}_n)/2] \times[\beta_C \delta_{mn} + (1-\delta_{mn})\beta_{1C} \cos\vec{k}\cdot(\vec{t}_m - \vec{t}_n)/2] , \quad (19)$$

$$H^{VC}_{mn}(\vec{k}) = H^{CV}_{mn}(\vec{k}) = 0 , \quad (20)$$

where

$$\beta_V = \langle \psi^b_m(\vec{r}) | H | \psi^b_m(\vec{r}) \rangle , \quad (21)$$

$$\beta_C = \langle \psi^a_m(\vec{r}) | H | \psi^a_m(\vec{r}) \rangle , \quad (22)$$

$$\beta_{1V} = \frac{1}{2(N_{bm}N_{bn})^{1/2}} [\langle \phi_m(\vec{r}) | H | \phi_n(\vec{r}) + \phi_n(-\vec{r}+\vec{t}_n) \rangle + (m \rightarrow n)] , \quad (23)$$

$$\beta_{1C} = -\frac{1}{2(N_{am}N_{an})^{1/2}} [\langle \phi_m(\vec{r}) | H | \phi_n(\vec{r}) - \phi_n(-\vec{r}+\vec{t}_n) \rangle + (m \rightarrow n)] . \quad (24)$$

The overlap integrals Δ_{mn}, $m \neq n$, are assumed to be zero.

The secular equation (14) can now be solved analytically for a general $\vec{k}$ point.[10] It gives the energies of the four valence-band states and the four conduction-band states in the form

$$\begin{aligned} E^V_1(\vec{k}) &= \beta_V + 2\beta_{1V}[1+S(\vec{k})] , \\ E^V_2(\vec{k}) &= \beta_V + 2\beta_{1V}[1-S(\vec{k})] , \\ E^V_3(\vec{k}) &= E^V_4(\vec{k}) = \beta_V - 2\beta_{1V} , \\ E^C_1(\vec{k}) &= E^C_2(\vec{k}) = -\beta_C - 2\beta_{1C} , \\ E^C_3(\vec{k}) &= -\beta_C + 2\beta_{1C}[1-S(\vec{k})] , \\ E^C_4(\vec{k}) &= -\beta_C + 2\beta_{1C}[1+S(\vec{k})] , \end{aligned} \quad (25)$$

where

$$S(\vec{k}) = (1 + \cos\tfrac{1}{2}k_x a \cos\tfrac{1}{2}k_y a + \cos\tfrac{1}{2}k_y a \cos\tfrac{1}{2}k_z a + \cos\tfrac{1}{2}k_z a \cos\tfrac{1}{2}k_x a)^{1/2} . \quad (26)$$

At $\vec{k}=0$, the valence-band width W_V, direct energy gap E_d, and the conduction-band width W_C can be written as

$$W_V = -8\beta_{1V} , \quad (27)$$

$$W_C = 8\beta_{1C} , \quad (28)$$

$$E_d = -(\beta_C + \beta_V) - 2\beta_{1C} + 2\beta_{1V} . \quad (29)$$

The energy-band structure is schematically shown in Fig. 2(b). At the Γ point, the top valence band is threefold degenerate and has Γ'_{25} symmetry. Similarly, the bottom of the conduction band is also threefold degenerate with Γ_{15} symmetry. Figure 2(c) corresponds to the case when β_{1C} changes sign, in which case the top nondegenerate conduction band (with Γ'_2 symmetry at $\vec{k}=0$) goes lower. The former situation occurs in the case of diamond and silicon, while the latter is observed in germanium. In Fig. 2(a), we have drawn the corresponding band structure in the localized bond approximation.

The valence-band structure thus obtained is quite close to that obtained from the more accurate pseudopotential method.[11] However, the conduction-band structure is not very satisfactory. However, since in our calculations it is perhaps necessary to know sufficiently well only some sort of average band structure over the whole BZ, we have used the above definite structure in calculating the nonresonant part of $\chi^{(3)}$ without making further approximations.

The eigenstates $|VM\vec{K}\rangle$ and $|CM\vec{K}\rangle$, $M=1,2,3,4$, corresponding to four valence bands and four conduction bands, can now be written as linear combinations of the functions $\Psi^V_m(\vec{k},\vec{r})$ and $\Psi^C_m(\vec{k},\vec{r})$, respectively, as

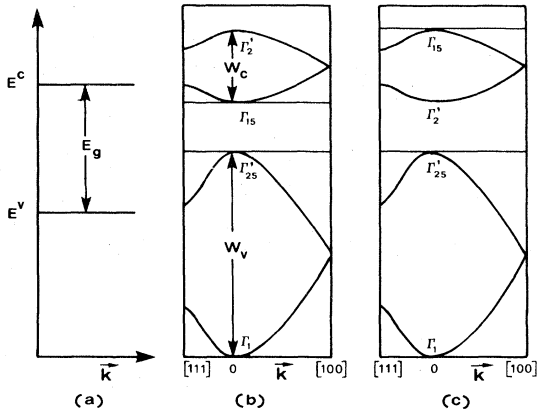

FIG. 2. Energy-band structure calculated in the tight-binding approximation in [100] and [111] directions for crystals with a diamond structure. (a) Completely localized band approximation, (b) and (c) when interactions between bonds having at least one atom common to them is taken into account.

$$|VM\vec{k}\rangle = \sum_m b_m^{VM}(\vec{k}) \exp(i\vec{k}\cdot\vec{t}_m)\Psi_m^V(\vec{k},\vec{r}), \quad (30)$$

$$|CM\vec{k}\rangle = \sum_m b_m^{CM}(\vec{k}) \exp(i\vec{k}\cdot\vec{t}_m)\Psi_m^C(\vec{k},\vec{r}). \quad (31)$$

These coefficients $b_m^{VM}(\vec{k})$ and $b_m^{CM}(\vec{k})$ can be calculated analytically by solving the secular equation (14) at any $\vec{k}$ point in the BZ.[12] However, we have determined them numerically in this work.

The dipole matrix elements between these states, which we shall need in our calculations, can also be written within this model as

$$\langle VM\vec{k}|\vec{r}|CN\vec{k}\rangle = -\sum_{m,n} b_m^{VM}(\vec{k})\, b_n^{CN}(\vec{k}) \frac{2}{(N_{bm}N_{an})^{1/2}} [(\vec{r}_{mn} - \tfrac{1}{2}\vec{t}_m\delta_{mn}) - \tfrac{1}{2}(\vec{r}'_{mn} - \vec{r}'_{nm})]\cos[\vec{k}\cdot(\vec{t}_m - \vec{t}_n)/2], \quad (32)$$

$$\langle VM\vec{k}|\vec{r}|VN\vec{k}\rangle = -i\sum_{m,n} b_m^{VM}(\vec{k})\, b_n^{VN}(\vec{k}) \frac{2}{(N_{bm}N_{bn})^{1/2}} [\vec{r}_{mn} + \tfrac{1}{2}(\vec{r}'_{mn} + \vec{r}'_{nm})]\sin[\vec{k}\cdot(\vec{t}_m - \vec{t}_n)/2], \quad (33)$$

$$\langle CM\vec{k}|\vec{r}|CN\vec{k}\rangle = -i\sum_{m,n} b_m^{CM}(\vec{k})\, b_n^{CN}(\vec{k}) \frac{2}{(N_{am}N_{an})^{1/2}} [\vec{r}_{mn} - \tfrac{1}{2}(\vec{r}'_{mn} + \vec{r}'_{nm})]\sin[\vec{k}\cdot(\vec{t}_m - \vec{t}_n)/2], \quad (34)$$

where

$$\vec{r}_{mn} = \langle \phi_m(\vec{r})|\vec{r}|\phi_n(\vec{r})\rangle, \quad (35)$$

$$\vec{r}'_{mn} = \langle \phi_m(\vec{r})|\vec{r}|\phi_n(-\vec{r}+\vec{t}_n)\rangle. \quad (36)$$

Note that these expressions for the dipole matrix elements have been written with respect to the midpoint θ (Fig. 1) of any one of the bonds as the origin of coordinate systems. This is because the crystal has a center-of-inversion symmetry about this point. Such a choice leads to a zero dipole moment in the ground state of the system. However, the choice of origin does not matter in the case of energy-band calculations.

III. NONLINEAR SUSCEPTIBILITY $\chi^{(3)}$

A general expression for $\chi^{(3)}$ can be derived by calculating the average value of induced polarization $\vec{P}$ in the ground state of the system, in the presence of electromagnetic fields, and then comparing it with Eq. (1). When the frequencies of the fields are small compared with typical band gaps, but large compared with resonant-phonon frequencies, the nondispersive part of the electronic $\chi^{(3)}$ is given by[1]

$$\chi_{ijkl}^{(3)} = 4e^4\,\mathrm{sym}(i,j,k,l) \times \sum_{mn}{}' \left(\sum_l{}' \frac{\langle g|r_i|m\rangle\langle m|r_j - \bar{r}_j|n\rangle\langle n|r_k - \bar{r}_k|l\rangle\langle l|r_l|g\rangle}{E_{mg}E_{ng}E_{lg}} - \frac{\langle g|r_i|m\rangle\langle m|r_j|g\rangle\langle g|r_k|n\rangle\langle n|r_l|g\rangle}{E_{mg}E_{ng}^2} \right), \quad (37)$$

where

$$\bar{r}_j = \langle g|r_j|g\rangle, \quad (38)$$

$$E_{mg} = E_m - E_g, \quad (39)$$

and the prime over the summation sign denotes that the ground state $|g\rangle$ is not included in the summation. The symbol $\mathrm{sym}(i,j,k,l)$ denotes symmetrization of the expression on the right with respect to i, j, k, and l. States and energies here refer to the complete many-particle electronic Hamiltonian of the solid.

Now at $T = 0$ °K, all the valence-band states are completely filled and conduction-band states are empty. The excited states m, n, l, etc. in Eq. (37) correspond to the situation in which one electron is put in any of the conduction bands. Neglecting possible interactions between the electron-hole pair (exciton effects), the above equation can be written in terms of single-particle Bloch states as[13]

$$\chi_{xxxx}^{(3)} = \frac{4e^4}{\Omega}\sum_{\vec{k}} \sum_{M,N,L,P} \left(\frac{\langle VM\vec{k}|x|CN\vec{k}\rangle\langle CN\vec{k}|x|CL\vec{k}\rangle\langle CL\vec{k}|x|CP\vec{k}\rangle\langle CP\vec{k}|x|VM\vec{k}\rangle}{E_{PM}^{CV}(\vec{k})E_{PN}^{CV}(\vec{k})E_{PL}^{CV}(\vec{k})} + \frac{\langle VM\vec{k}|x|VN\vec{k}\rangle\langle VN\vec{k}|x|VL\vec{k}\rangle\langle VL\vec{k}|x|CP\vec{k}\rangle\langle CP\vec{k}|x|VM\vec{k}\rangle}{E_{PM}^{CV}(\vec{k})E_{PN}^{CV}(\vec{k})E_{PL}^{CV}(\vec{k})} - \frac{\langle VM\vec{k}|x|VN\vec{k}\rangle\langle VN\vec{k}|x|CL\vec{k}\rangle\langle CL\vec{k}|x|CP\vec{k}\rangle\langle CP\vec{k}|x|VM\vec{k}\rangle}{E_{LM}^{CV}(\vec{k})E_{LN}^{CV}(\vec{k})E_{PM}^{CV}(\vec{k})} - \frac{\langle VM\vec{k}|x|VN\vec{k}\rangle\langle VN\vec{k}|x|CL\vec{k}\rangle\langle CL\vec{k}|x|CP\vec{k}\rangle\langle CP\vec{k}|x|VM\vec{k}\rangle}{E_{PN}^{CV}(\vec{k})E_{PM}^{CV}(\vec{k})E_{LN}^{CV}(\vec{k})} - \frac{\langle VM\vec{k}|x|CN\vec{k}\rangle\langle CN\vec{k}|x|VL\vec{k}\rangle\langle VL\vec{k}|x|CP\vec{k}\rangle\langle CP\vec{k}|x|VM\vec{k}\rangle}{E_{NM}^{CV}(\vec{k})E_{NL}^{CV}(\vec{k})E_{PM}^{CV}(\vec{k})} \right), \quad (40)$$

$$E^{CV}_{NM}(\vec{k}) = E^{C}_{N}(\vec{k}) - E^{V}_{M}(\vec{k}) . \quad (41)$$

Note that in the completely localized bond approximation, $\beta_{1V} = \beta_{1C} = 0$, so that the valence and conduction bands are fourfold degenerate with constant energy difference E_g. The corresponding wave functions are given by Eqs. (11) and (12), and Eq. (40) in that case reduces to

$$\chi^{(3)}_{xxxx} = \frac{4e^4 N}{E_g^3} \sum_m \{ |\langle \psi^b_m(\vec{r}) | x | \psi^a_m(\vec{r}) \rangle|^2 [\langle \psi^a_m(\vec{r}) | x | \psi^a_m(\vec{r}) \rangle - \langle \psi^b_m(\vec{r}) | x | \psi^b_m(\vec{r}) \rangle]^2 - |\langle \psi^b_m(\vec{r}) | x | \psi^a_m(\vec{r}) \rangle|^4 \} . \quad (42)$$

For crystals with center-of-inversion symmetry, the first term is identically zero, while the second term is nonzero and negative. To obtain positive values for $\chi^{(3)}$, one must go beyond the completely localized bond approximation discussed earlier.

We make explicit calculations of $\chi^{(3)}$ given by Eq. (40), with the dipole matrix elements given by Eqs. (32)–(34) and the energy values given by Eq. (25). For this, we first need to fix the energy parameters β_V, β_C, β_{1V}, and β_{1C}. These four parameters actually reduce to three by taking the top of the valence band as the zero of the energy scale. Two parameters are fixed by using Eqs. (27) and (29) with the known experimental values of W_V and E_d. To fix the third parameter, we calculate the linear dielectric constant ϵ_{xx} in this model. This can be written as

$$\epsilon_{xx} = 1 + \frac{4\pi e^2}{\Omega} \sum_{\vec{k}} \sum_{M,N} \frac{|\langle VM\vec{k} | x | CN\vec{k} \rangle|^2}{E^{CV}_{MN}(\vec{k})} . \quad (43)$$

When this is compared with the corresponding experimental value, the third parameter gets fixed completely.

For calculating the dipole matrix elements, we have taken the explicit form of the s- and p-type atomic orbitals as

$$\phi_s(r) = re^{-\alpha_1 r} , \quad (44)$$

$$\phi_x(r) = xre^{-\alpha_2 r} , \quad (45)$$

and so on, where α_1 and α_2 are known constants. This form of the atomic orbitals has been recently used successfully by Chadi[9] in his more elaborate tight-binding calculations of energy-band structure of group-IV crystals. In the explicit form of the s- and p-type atomic orbitals for Si and Ge, our values of α_1 and α_2 (1.6 and 1.8, respectively) are only slightly different from those used by Chadi[9] ($\alpha_1 = \alpha_2 = 1.7$). In our case, in these crystals, $S_{mm} \sim 0.85$, while $S_{mn} \sim 0.1$ for $m \neq n$. This justifies the neglect of the overlaps Δ_{mn}, $m \neq n$ in Eq. (14). Similarly, in the case of diamond, for which there are no calculations by Chadi, we have taken α_1 and α_2 to be 1.5 and 1.8, respectively.

Using the above procedure, we have calculated $\chi^{(3)}$ in diamond, silicon, and germanium. The summation over $\vec{k}$ in the BZ in Eqs. (40) and (43) is done by dividing it into small cubic meshes and making use of the 48-fold symmetry of the cubic group for the BZ. The different parameters used in our calculations for all these crystals are given in Table I. The values of the dipole matrix elements [Eqs. (35) and (36)] between any two bonding orbitals are also given there. We have listed four such dipole matrix elements $\vec{r}_{mm} \cdot \hat{t}_m$, $\vec{r}_{mn} \cdot \hat{t}_m = \vec{r}_{mn} \cdot \hat{t}_n$, $\vec{r}'_{mn} \cdot \hat{t}_m$, and $\vec{r}'_{mn} \cdot \hat{t}_n$, ($\vec{r}'_{mn} \sim 0$) in either of the bonding directions, where each one is the same for all values of m and n because of the cubic symmetry

TABLE I. Calculated and experimental values of macroscopic χ^3_{xxxx} for diamond, silicon, and germanium. Other parameters used in these calculations are also given. In column 10, values of the linear dielectric constant ϵ_{xx} calculated in this model are given with the experimental values in parentheses.

	W_V (eV)	E_d (eV)	W_C (eV)	$\vec{r}_{mm} \cdot \hat{t}_m$ (Å)	$\vec{r}_{mn} \cdot \hat{t}_m = \vec{r}_{mn} \cdot \hat{t}_n$ (Å)	$\vec{r}'_{mn} \cdot \hat{t}_n$ (Å)	$\vec{r}'_{mn} \cdot \hat{t}_n$ (Å)	S	ϵ_{xx}	χ^3_{xxxx} (10^{-12} esu) Theory	Experiment
Diamond ($\alpha_1 = 1.5$, $\alpha_2 = 1.8$)	20.0	5.0	4.7	0.45	0.151	0.25	−0.20	0.87	5.8 (5.9)	0.043	0.046 ± 0.006 [a]
Silicon ($\alpha_1 = 1.6$, $\alpha_2 = 1.8$)	12.7	3.2	4.3	0.71	0.237	0.02	−0.21	0.85	12.2 (12.0)	2.62	6.0 ± 3.0 [b]
Germanium ($\alpha_1 = 1.6$, $\alpha_2 = 1.8$)	12.7	1.0	3.5	0.74	0.248	0.02	−0.22	0.85	16.2 (16.0)	6.7	100.0 ± 50.0 [b]

[a] M. D. Levenson and N. Bloembergen, Phys. Rev. B 10, 4447 (1974).
[b] J. J. Wynne and G. D. Boyd, Appl. Phys. Lett. 12, 191 (1968).

of the crystal. The dipole matrix element in any other direction can easily be calculated in terms of these four values using symmetry properties. We have also given the calculated values of the linear dielectric constant in the table, with experimental values in brackets. Except for the case of Ge, the values of $\chi^{(3)}$ thus obtained are in reasonably good agreement with the experimental results. As expected, the best agreement is for the case of diamond, which is most tightly bound.

IV. DISCUSSION AND CONCLUDING REMARKS

Using the tight-binding bonding orbital approach for the electronic band structure, we have shown that it is necessary to include bond-bond interaction for calculating $\chi^{(3)}$ in group-IV crystals. By including interactions up to nearest-neighbor bonds only, we have obtained reasonable results for the nonresonant part of $\chi^{(3)}$ in diamond and silicon. For Ge, the agreement is poor. We shall discuss this trend a little later. Note also that we have not included direct local-field corrections to $\chi^{(3)}$ in any of these cases.

In our procedure, the various energy parameters have been fixed self-consistently from other experimentally known quantities, e.g., valence-band width at $\vec{k}=0$, the direct energy gap, and the linear dielectric constant. Bonding orbitals which are used to construct tight-binding wave functions are constructed from the hybridized sp^3 orbitals. To have a further check on the values of various parameters used in our calculations, we also verified the oscillator f-sum rule for the valence bands. The sum rule states that[14]

$$\frac{2m}{\hbar^2}\sum_{\vec{k}}\sum_{N}|\langle VM\vec{k}|\vec{r}|CN\vec{k}\rangle|^2 E_{NM}^{CV}(\vec{k})=2N/\Omega \tag{46}$$

for each of the valence bands. This relation is found to be satisfied within 10% for the top three bands for silicon, germanium, and diamond. For the lowest valence band the error is slightly higher, but its contribution to both $\chi^{(1)}$ and $\chi^{(3)}$ is almost negligible because of large energy denominators.

Table I shows that the calculated and experimental values of $\chi^{(3)}$ for diamond are in excellent agreement. For Si, $\chi^{(3)}$ is slightly lower than the experimental value. For Ge, the calculated value is considerably lower than the experimental value. This gradual deviation of our tight-binding $\chi^{(3)}$ from the experimental values as we go from diamond to germanium shows the inadequacy of the simple tight-binding model for heavier elements. This is because of the fact that we have completely neglected the effects of the d-electron states in constructing our bonding orbitals, which become quite important in Ge, and also our neglect of interactions beyond the nearest-neighbor bonds. It has been pointed out by Chadi[9] that when d electrons are not included in the construction of tight-binding states, it is necessary to take s and p orbitals to be more delocalized for representing Bloch functions in the crystal. This implies that the interactions beyond nearest-neighbor bonds become important. In any case, it is gratifying to note that the tight-bonding method works best for the case of diamond, where it should. For small-gap semiconductors, the calculation of $\chi^{(3)}$ via the intraband Franz-Keldysh contribution as discussed by Van Vechten and Aspnes[6] may become more relevant.

ACKNOWLEDGMENTS

One of the authors (K.A.) would like to thank Professor Abdus Salam, the International Atomic Energy Agency, and UNESCO for hospitality at the International Center for Theoretical Physics, Trieste.

*Present address: Max-Planck-Institut für Festkörperforschung, 7000 Stuttgart 80, Fed. Rep. Germany.

[1]S. S. Jha and N. Bloembergen, Phys. Rev. 171, 891 (1968).
[2]J. C. Phillips and J. A. Van Vechten, Phys. Rev. 183, 709 (1969).
[3]D. A. Kleinman, Phys. Rev. B 2, 3139 (1970); C. L. Tang and C. Flytzanis, Phys. Rev. B 4, 2520 (1971); B. F. Levine, Phys. Rev. B 7, 2600 (1973); K. Arya and A. V. Tankhiwale, Pramana 4, 38 (1975).
[4]C. Flytzanis, Phys. Lett. A 31, 273 (1970).
[5]C. A. Coulson, *Valence*, 2nd ed. (Oxford University, London, 1961); C. A. Coulson, L. B. Redei, and D. Stocker, Proc. R. Soc. A 270, 357 (1962).
[6]J. A. Van Vechten and D. E. Aspnes, Phys. Lett. A 30, 346 (1969); J. A. Van Vechten, M. Cardona, D. E. Aspnes, and R. M. Martin, in *Proceedings of the Tenth International Conference on the Physics of Semiconductors*, Cambridge, Mass., 1970, edited by S. P. Keller, J. C. Hensel, and F. Stern (USAEC Division of Technical Information Extension, Oak Ridge, Tennessee, 1970), p. 82.
[7]G. Leman and J. Friedel, J. Appl. Phys. Suppl. 33, 281 (1962).
[8]W. A. Harrison, Phys. Rev. B 8, 4487 (1973); W. A. Harrison and S. Ciraci, Phys. Rev. B 10, 1516 (1974).
[9]D. J. Chadi, Phys. Rev. B 16, 3572 (1977).
[10]D. Stocker, Proc. R. Soc. A 270, 397 (1962).
[11]D. Brust, Phys. Rev. A 134, 1337 (1964).
[12]K. Arya, Ph.D. thesis (Bombay University, 1975) (unpublished).
[13]Note that in the transport region, there are only two independent components of $\chi^{(3)}_{ijkl}$ for these crystals: $\chi^{(3)}_{xxxx}$ and $\chi^{(3)}_{xxyy}$, with $3\chi_{xxyy}\approx\chi_{xxxx}$ for spherical bands.
[14]D. Pines, *Elementary Excitations in Solids* (Benjamin, New York, 1963).